Geophysical Research Letters

RESEARCH LETTER
10.1029/2020GL088550

# Eddy Kinetic Energy in the Arctic Ocean From a Global Simulation With a 1-km Arctic

Qiang Wang[1,2], Nikolay V. Koldunov[1,3], Sergey Danilov[1,4,5], Dmitry Sidorenko[1], Claudia Wekerle[1], Patrick Scholz[1], Igor L. Bashmachnikov[6,7], and Thomas Jung[1,8]

[1]Alfred-Wegener-Institut Helmholtz-Zentrum für Polar- und Meeresforschung (AWI), Bremerhaven, Germany, [2]Laboratory for Regional Oceanography and Numerical Modeling, Qingdao National Laboratory for Marine Science and Technology, Qingdao, China, [3]MARUM—Center for Marine Environmental Sciences, Bremen, Germany, [4]Department of Mathematics and Logistics, Jacobs University, Bremen, Germany, [5]A. M. Obukhov Institute of Atmospheric Physics, Russian Academy of Science, Moscow, Russia, [6]Department of Oceanography, The Saint Petersburg State University, St. Petersburg, Russia, [7]Nansen International Environmental and Remote Sensing Centre, St. Petersburg, Russia, [8]Institute of Environmental Physics, University of Bremen, Bremen, Germany

**Key Points:**
- A decadal-scale global simulation with the whole Arctic Ocean at 1-km resolution is carried out using FESOM2
- A basinwide overview of Arctic eddy energetics is provided with a focus on spatial patterns and seasonal changes of eddy kinetic energy
- Continental slopes in southern Canada and eastern Eurasian basins are the most energetic regions featuring similar seasonality

**Supporting Information:**
- Supporting Information S1

**Correspondence to:**
Q. Wang,
Qiang.Wang@awi.de

**Citation:**
Wang, Q., Koldunov, N. V., Danilov, S., Sidorenko, D., Wekerle, C., Scholz, P., et al. (2020). Eddy kinetic energy in the Arctic Ocean from a global simulation with a 1-km Arctic. *Geophysical Research Letters*, *47*, e2020GL088550. https://doi.org/10.1029/2020GL088550

Received 22 APR 2020
Accepted 23 JUN 2020
Accepted article online 8 JUL 2020



**Abstract** Simulating Arctic Ocean mesoscale eddies in ocean circulation models presents a great challenge because of their small size. This study employs an unstructured-mesh ocean-sea ice model to conduct a decadal-scale global simulation with a 1-km Arctic. It provides a basinwide overview of Arctic eddy energetics. Increasing model resolution from 4 to 1 km increases Arctic eddy kinetic energy (EKE) and total kinetic energy (TKE) by about 40% and 15%, respectively. EKE is the highest along main currents over topography slopes, where strong conversion from available potential energy to EKE takes place. It is high in halocline with a maximum typically centered in the depth range of 70–110 m, and in the Atlantic Water layer of the Eurasian Basin as well. The seasonal variability of EKE along the continental slopes of southern Canada and eastern Eurasian basins is similar, stronger in fall and weaker in spring.

**Plain Language Summary** Ocean mesoscale eddies play crucial roles in the ocean, climate, and ecosystem. While this is presumably also true for Arctic eddies, their dynamics and impacts are far less understood than for lower latitudes: It is a great challenge to resolve the very small Arctic eddies in numerical simulations. Just now, owing to the development of new-generation models, it becomes possible to resolve Arctic eddies in realistic global ocean configurations. The study presents the results from a first-ever decadal-scale global simulation with the Arctic Ocean at 1-km resolution. An overview of the eddy kinetic energy and its generation is provided for the Arctic deep basin, with a focus on both spatial and seasonal variability. The current results fill some knowledge gaps in Arctic eddy energetics, and also help to identify questions that we will be able to answer with such frontier simulations in the future.

## 1. Introduction

Mesoscale eddies have been observed at various depths for different basins of the Arctic Ocean (e.g., Bashmachnikov et al., 2020; D'Asaro, 1988; Dmitrenko et al., 2008; Manley & Hunkins, 1985; Muench et al., 2000; Nishino et al., 2011; Kawaguchi et al., 2012; Kozlov et al., 2019; Padman et al., 1990; Pnyushkov et al., 2018; Timmermans et al., 2008; Woodgate et al., 2001; Zhao et al., 2014, 2016). They might influence the ocean, climate, and ecosystem in various ways. In the Eurasian Basin, mesoscale eddies can propagate over long distances, with possible impacts on vertical mixing and ocean stratification over large spatial scales (Pnyushkov et al., 2018; Woodgate et al., 2001). In the Canada Basin, eddy fluxes, together with the feedback effect of ocean surface geostrophic currents caused by sea ice, tend to stabilize the Beaufort Gyre and influence the storage of fresh water (Armitage et al., 2020; Manucharyan & Spall, 2016; Meneghello et al., 2017; Wang, Marshall, et al. 2019). Furthermore, eddies play an important role in the ventilation of the Arctic halocline (Pickart et al., 2005; Spall et al., 2008) and transport of biological species from continental shelves to adjacent deep basins (Watanabe et al., 2014).

Despite the crucial role of eddies, there are still major knowledge gaps in our understanding of their properties and dynamics in the Arctic Ocean. For example, eddy kinetic energy (EKE) was found to be about one third of the total kinetic energy (TKE) in the upper 200 m of the Canada Basin based on 127 eddies observed from ice drift camps (Manley & Hunkins, 1985); however, it remains unknown how representative this value

is for other Arctic regions. In fact, available eddy observations in the Arctic Ocean are still very sparse. This calls for eddy-resolving numerical simulations to complement observations for studying Arctic eddies.

In the past, EKE inside the Arctic Ocean has been discussed based on model simulations with 9 km (Maslowski et al., 2008) and 3–4 km (Regan et al., 2020) resolutions. The analysis of Maslowski et al. (2008) suggested that resolution of the order of a few kilometers is at least needed to fully represent eddy energetics in the Arctic Ocean. Indeed, the typical radius of observed halocline eddies in the probability distribution shows two peaks centered around 4 and 7 km for Canadian water eddies and a peak centered around 4.5 km for Eurasian water eddies (Zhao et al., 2014). The smallness of eddies makes eddy-resolving simulations a computationally very challenging task. Considering that simulated variance at scales smaller than 10 times of the model grid size is typically damped due to numerical dissipation (Soufflet et al., 2016), one might even need 1-km grid size to resolve the small eddies in the Arctic Ocean. This requires tremendous computational resources along with scalable models, which can make effective use of these resources.

In this paper we present the first Arctic-wide analysis of eddy energetics, exploiting a novel 10-year long global simulation in which the whole Arctic Ocean is represented with a resolution of 1 km. More specifically, we will investigate the spatial and seasonal variability of the EKE over the Arctic basin.

## 2. Model Setup

We employ unstructured-grid Finite volumE Sea ice Ocean Model version 2 (FESOM2), which allows the use of variable resolution without the need for nesting (Danilov et al., 2017). Its predecessor FESOM1 (Wang et al., 2014) has been widely used in Arctic studies with horizontal resolution of about 4 km (e.g., Wang et al., 2016, 2020; Wang, Wekerle, Danilov, Koldunov, et al., 2018; Wang, Wekerle, et al., 2019; Wekerle et al., 2017). The performance of FESOM2 is very similar to its predecessor in terms of the simulated ocean and sea ice states (Scholz et al., 2019); however, it is computationally much more efficient (up to 5 times speedup, Koldunov, Aizinger, et al., 2019; Scholz et al., 2019), thus allowing to use higher model resolution with the same available computational resources at very high throughput. The model's sea ice component is discretized on the same unstructured grid as the ocean component (Danilov et al., 2015). It can faithfully reproduce sea ice observations, including sea ice linear kinematic features when using high model resolution (Koldunov, Danilov, et al., 2019; Wang et al., 2016).

The model horizontal resolution is 30 km in the global ocean, except for the Arctic Ocean, where the resolution is 1 km (call Exp1km, Figure S1 in the supporting information). In the vertical, 70 $z$ levels are used. The model is driven by the atmospheric reanalysis fields from JRA55-do v.1.4 (Tsujino et al., 2018). It was initialized from PHC3 climatology (Steele et al., 2001) starting from the year 2000 and has been run for 10 years. Here we analyze the last five model years. To assess the impact of horizontal resolution on the representation of mesoscale eddies, another simulation was carried out. It is the same as Exp1km, except for using a 4-km resolution inside the Arctic Ocean (called Exp4km).

The TKE is calculated online during the model run as TKE = $(u^2+v^2)/2$, where $u$ ($v$) is three-dimensional zonal (meridional) velocity evolving with time. By separating the velocity to its mean value and anomaly, $u = \bar{u} + u'$, $v = \overline{v} + v'$, TKE can be decomposed to the mean kinetic energy (MKE, energy associated with the mean current) and the EKE:

$$\mathrm{TKE} = (\bar{u}^2 + \bar{v}^2)/2 + (u'^2 + v'^2)/2 = \mathrm{MKE} + \mathrm{EKE} \quad (1)$$

We saved monthly mean velocity and TKE from the model, which are then used to calculate EKE. If annual mean data were used to compute EKE, it would contain the component associated with seasonal variability of the mean currents, so we used monthly mean data in the calculation. In this paper we calculate and study the mean TKE and EKE averaged over the last five model years and the mean seasonality over this period.

## 3. Results

### 3.1. Impacts of Model Resolution

As revealed by the snapshots of relative vorticity in the Beaufort Sea, numerous eddies are present in the 1-km simulation (Figure 1a). In contrast, the 4-km simulation is dominated by large meanders rather

than eddies (Figure 1b). Although some features look like eddies with circular shapes on this coarser mesh, they are much larger in size than the eddies resolved with 1-km resolution. In the Eurasian Basin, the 4-km run is only eddy-permitting, as eddies are not so well represented as in the 1-km run (Figures 1c–1f). The comparison confirms that the grid size of 4 km, which is fine enough to properly resolve mesoscale eddies in midlatitudes, is insufficient for the Arctic Ocean. This is not surprising, as the first baroclinic Rossby deformation radius (Nurser & Bacon, 2014) and the radii of observed mesoscale eddies (on the order of a few kilometers, Zhao et al., 2014) are very small in the Arctic Ocean. An additional 5-year sensitivity experiment at 2-km resolution simulates some well-defined eddies, but fewer than the 1-km run does. Therefore, we argue that *at least* a 1-km grid size is required to resolve eddies in the Arctic basin.

Resolving the mesoscale eddies leads to a more energetic Arctic basin. The total EKE (total TKE) integrated over the Arctic deep basin (area with topography deeper than 500 m) and averaged over the last five model years is 40% (15%) higher in Exp1km than in Exp4km. It is important to notice that the EKE, as decomposed in (1), consists of the component associated with meanders when they are present. Therefore, the computed EKE from Exp4km is still significant, although eddies are not well simulated. The EKE in Exp4km is very similar to that in a simulation using 3–4-km resolution analyzed by Regan et al. (2020) (The EKE diagnosed as they did is shown and explained in Figure S2). In the following, we will investigate the spatial and seasonal variation of Arctic EKE in the 1-km resolution simulation.

### 3.2. Spatial Variation of EKE

The spatial pattern of the TKE vertically integrated over the upper 200 m in the 1-km resolution run is shown in Figure 2a. The first thing to notice is that the currents along bottom topography slopes are more energetic than those in the interior ocean. This spatial pattern highlights the point that key features of the Arctic Ocean circulation are shaped by bottom topography. The Eurasian Basin is characterized by the strong cyclonic Arctic Circumpolar Boundary Current (ACBC, Aksenov et al., 2011), which splits into two branches when reaching the Lomonosov Ridge (Woodgate et al., 2001). In the Amerasian Basin, the most outstanding feature is the energetic Beaufort/Chukchi shelfbreak jet. The central Beaufort Gyre also possesses relatively high TKE.

Overall, the spatial pattern of the vertically integrated EKE is very similar to the TKE (Figure 2b). This indicates that eddies are most active along the bottom slopes, where the main currents are located. The strength of EKE decreases from the continental slopes and the Lomonosov Ridge toward the basin interior. Inside the Amerasian Basin, the Beaufort Gyre has higher EKE than other areas. The EKE is a significant part of the TKE (Figure 2c). An observational estimate suggests that EKE is about one third of the TKE averaged in the Canada Basin (Manley & Hunkins, 1985), which is consistently represented by the model. The model result reveals that the ratio EKE/TKE varies significantly in space, largely in the range of 10–60%. In the central Eurasian Basin and Beaufort Gyre, the MKE is low and EKE accounts for more than 60% of the TKE. Integrated over the whole Arctic deep basin, EKE amounts to 36% of the TKE.

The vertical profiles of EKE for a number of selected locations are shown in Figure 2d. There is an EKE maximum in the halocline in the Beaufort Gyre and along the Alaskan continental slope, centered at about 70–110 m depth. This is similar to the eddy core depth observed in the Canadian water (Zhao et al., 2014). Over the continental slope in the eastern Eurasian Basin, the EKE either has a maximum in the Atlantic Water layer or has similarly large values in both the halocline and the Atlantic Water layer. The latter is consistent with the observed collocation of eddy activity in the two layers (Pnyushkov et al., 2018; Woodgate et al., 2001).

As suggested by the vertical profiles of EKE, it is interesting to investigate the EKE in both the halocline and Atlantic Water layer. Although mesoscale eddies are observed in the Arctic halocline in different basins (Zhao et al., 2014), it turns out that eddies at the halocline depth are the most energetic along and close to topography slopes (Figure 3a). On the side of the Eurasian Basin, the EKE at 80 m is the highest in the West Spitsbergen Current (WSC), which is occupied by warm saline Atlantic Water, not Arctic halocline water. The simulated mean EKE in WSC is within the range (50–200 $cm^2\ s^{-2}$) observed by von Appen et al. (2016). Throughout the Eurasian Basin the EKE at 80 m is relatively high (Figure 3a). In the Amerasian Basin, the strongest EKE is along the Beaufort/Chukchi shelfbreak jet. On average, the EKE at 80 m depth

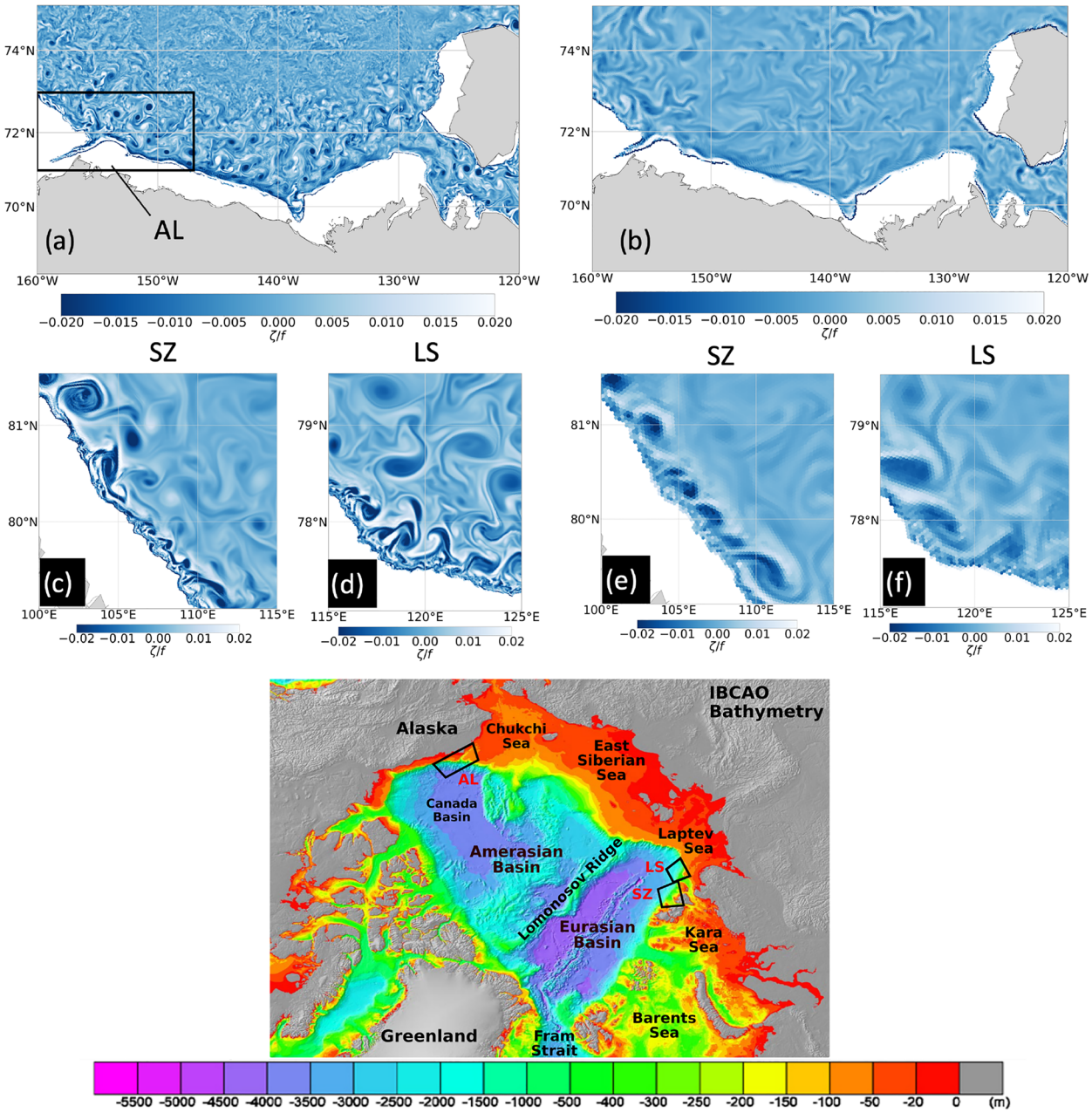


**Figure 1.** Snapshots of relative vorticity in the two simulations. (a) Beaufort Sea at 100-m depth in the 1-km resolution simulation. (b) The same as (a), but in the 4-km resolution simulation. (c) A region north of Severnaya Zemlya (SZ) and (d) a region north of Laptev Sea (LS) at 500-m depth in the 1-km simulation. (e, f) The same as (c, d), but in the 4-km simulation. In (a), the black box indicates the Alaskan region (AL) analyzed in the paper, and the regions shown in (c) and (d) correspond to the two regions in the Eurasian Basin analyzed in the paper. These regions are indicated by black boxes in the bottom panel, which shows the Arctic bathymetry from IBCAO (Jakobsson et al., 2012).

in the interior of the Amerasian Basin is weaker than in the interior of the Eurasian Basin, except for the central Beaufort Gyre.

Analysis of our model results shows that the mean conversion from eddy available potential energy to EKE through baroclinic instability is typically much higher than that from mean kinetic energy within the Arctic Ocean (not shown). Observations in a few limited regions have suggested the same (Pickart et al., 2005; Pnyushkov et al., 2018; Spall et al., 2008; Timmermans et al., 2008; Woodgate et al., 2001). Figure 3c shows the baroclinic conversion $\mathrm{BCC} = \overline{w'b'}$ (Harrison & Robinson, 1978) integrated over the upper 200 m, where $w$

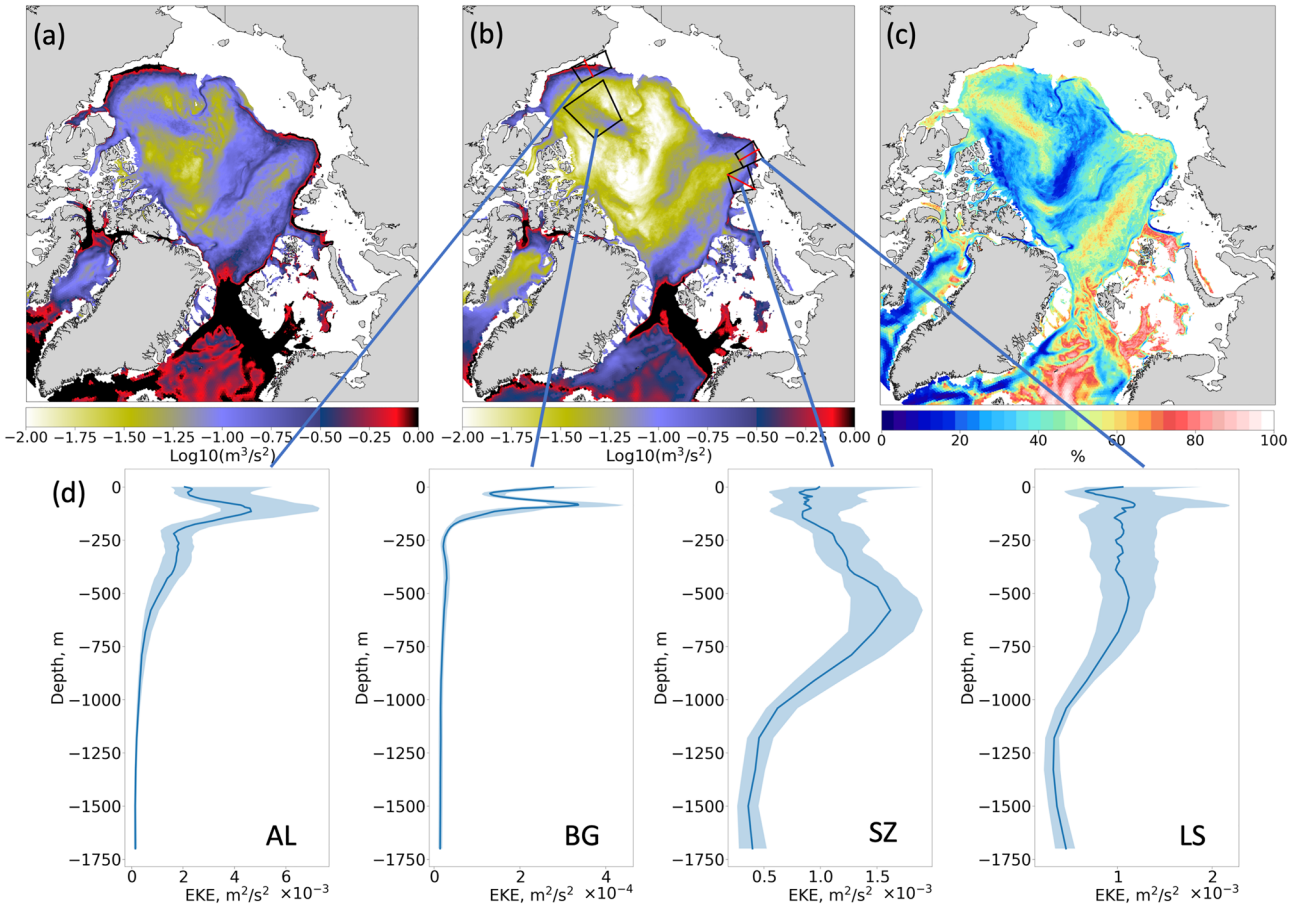


**Figure 2.** (a) Total kinetic energy (TKE) vertically integrated over the upper 200 m in the 1-km resolution simulation. (b) The same as (a), but for the eddy kinetic energy (EKE). (c) The ratio between vertically integrated EKE and TKE over the upper 200 m (in %). (d) Vertical profiles of EKE averaged in four chosen regions (indicated in (b)). Results are based on averages over the last five model years; the same in the following figures. The locations of transects shown in Figure 4 are indicated by red lines in (b). AL, Alaskan coast; BG, Beaufort Gyre; SZ, Severnaya Zemlya; LS, Laptev Sea.

is vertical velocity, $b = -g\rho/\rho_0$ is buoyancy, and $\rho_0 = 1{,}027$ kg m$^{-3}$. The prime denotes the anomaly from the monthly means. Consistent with the spatial pattern of EKE (Figure 3a), the BCC is stronger over the continental slopes in both basins (Figure 3c), indicating that the majority of the EKE originates from baroclinic instability of boundary currents. The BCC is also relatively strong along the Lomonosov Ridge, which explains the relatively strong EKE there.

The Beaufort Gyre in the Canada Basin is a freshwater reservoir sustained by Ekman convergence and downwelling driven by predominant anticyclonic winds in this region (Proshutinsky et al., 2009). Increases in available potential energy associated with freshwater accumulation and steepening of isopycnals are counteracted by eddy dissipation (Manucharyan & Spall, 2016). A recent study by Armitage et al. (2020) suggests enhanced eddy generation in the Beaufort Gyre in response to increased available potential energy induced by stronger wind power input. Our simulation consistently shows that eddies present in the Beaufort Gyre can have an origin from baroclinic instability inside the basin as indicated by relatively high BCC, in addition to eddies propagated to the basin from boundary currents.

The EKE at 500-m depth, representing the Arctic Atlantic Water layer, is lower than that at 80-m depth at most of the locations (cf. Figures 3a and 3b). An exception is the continental slope north of Severnaya Zemlya (SZ), where the EKE at 500-m depth is even higher than that in the halocline (see also Figure 2d). This can be explained by enhanced baroclinic instability after the two branches of Atlantic Water inflow, the Barents and Fram Strait branches, join together north of the Kara Sea (Dmitrenko et al., 2015), which causes strong conversion from available potential energy to EKE (Figure 3d). Previous studies showed

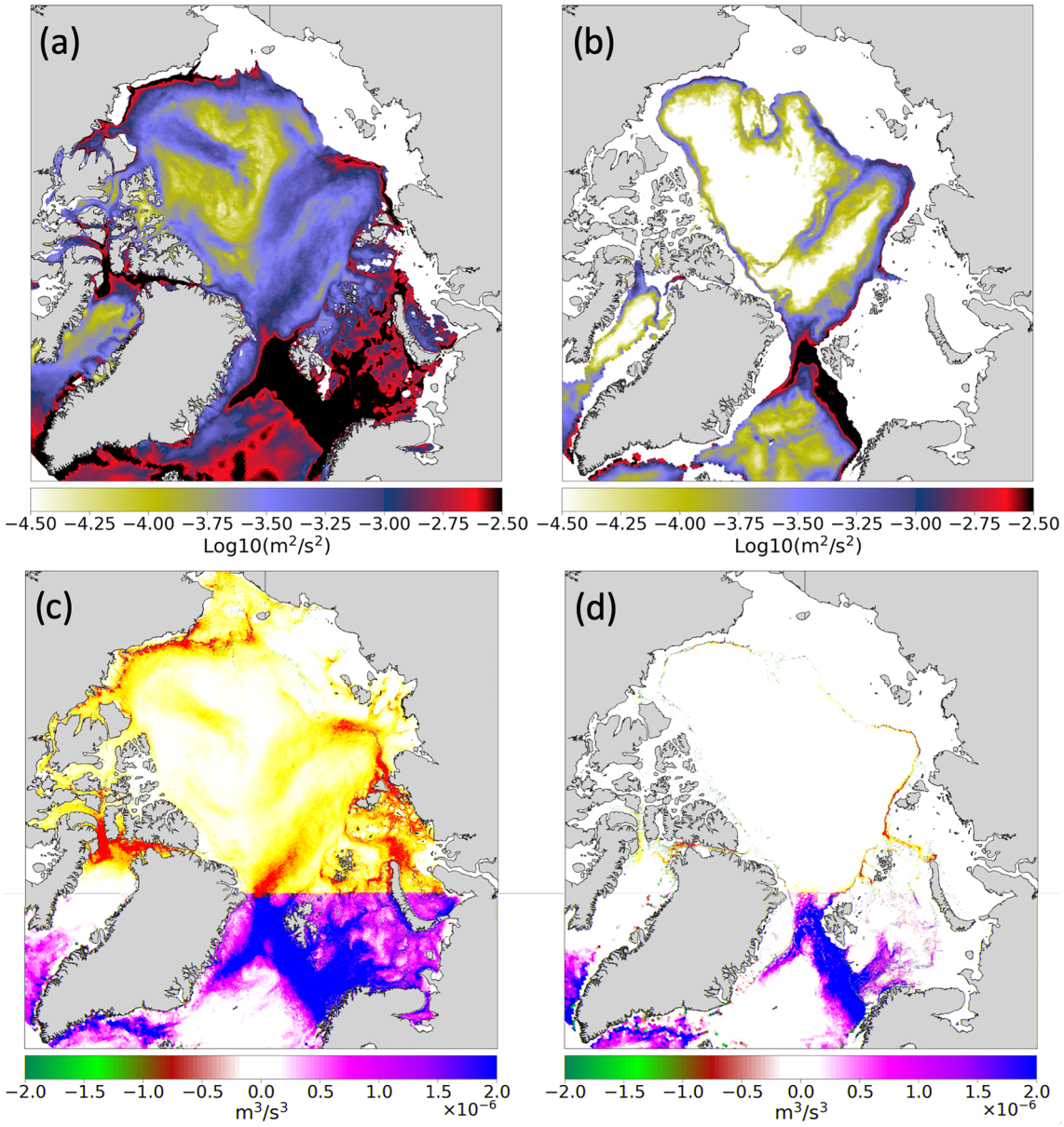


**Figure 3.** Eddy kinetic energy (EKE) at (a) 80 m and (b) 500 m in the 1-km resolution simulation. The energy conversion between available eddy potential energy and EKE ($\overline{w'b'}$) integrated over the depth range (c) 0–200 m and (d) 200–500 m. The vertically integrated EKE for these two depth ranges is shown in Figure S3 in the supporting information.

that the Barents Sea branch of Atlantic Water enhances the seasonal variability of the boundary current in the Eurasian Basin (Dmitrenko et al., 2009; Lique & Steele, 2012; Wang, Wekerle, Danilov, Wang, et al., 2018). The results from our eddy-resolving simulations suggest that this branch also increases the baroclinic instability and the EKE. Along the bottom topography slope north of the Chukchi Borderland, there is relatively high EKE in the Atlantic Water layer (Figure 3b) and in the lower halocline (not shown). The eddy generation can be related to the confluence of the Pacific and Atlantic waters and the complex bottom topography in this region (Woodgate et al., 2007).

The vertical transect along 152°W depicts the EKE structure across the Alaskan continental slope (Figure 4a). Strong EKE extends from the upper slope toward the Beaufort Sea and its value decreases with depth and distance from the shelf. The energy conversion term BCC has the largest value at the upper slope (Figure 4b), collocated with the strongest EKE. The spatial structure of the EKE and BCC indicates that

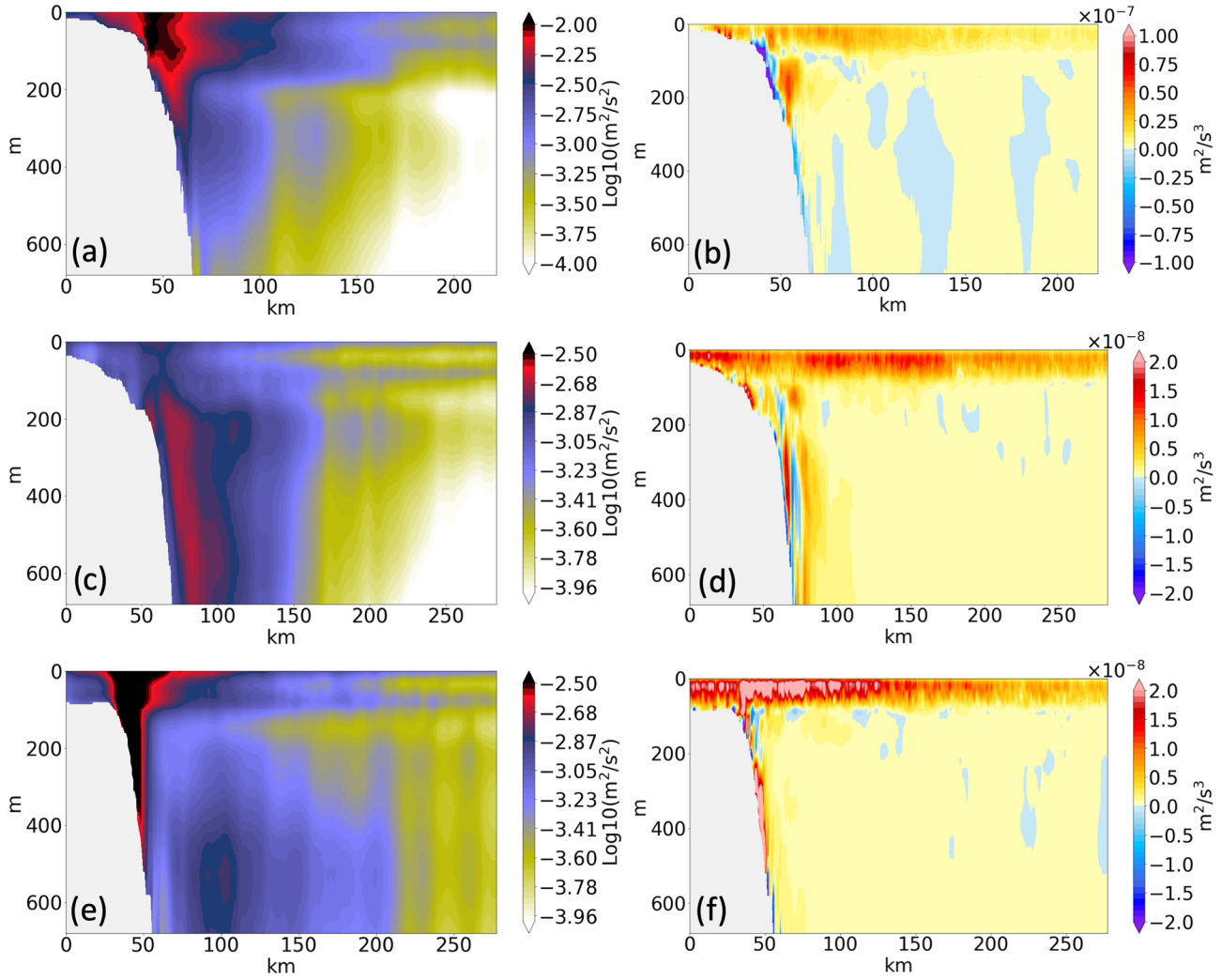


**Figure 4.** Vertical transects of (left) eddy kinetic energy (EKE) and (right) the baroclinic energy conversion ($\overline{w'b'}$): (a, b) along 152°W off the Alaskan coast; (c, d) north of Severnaya Zemlya; (e, f) north of Laptev Sea. The locations of the transects are indicated by red curves in Figure 2b. Color scales are different for different transects.

eddies are formed from the instability of the shelfbreak jet as suggested by observations (Pickart et al., 2005; Spall et al., 2008; von Appen & Pickart, 2012). The magnitude of mean BCC in this transect is about $6\times10^{-8}$ $m^2\,s^{-3}$ (varying in the range of $2\times10^{-8}$ to $2\times10^{-7}$ $m^2\,s^{-3}$ seasonally), consistent with the values suggested by observations (Spall et al., 2008; von Appen & Pickart, 2012). High EKE occupies a larger lateral extent than BCC, indicating that eddies are shed off from the shelf break toward the deep basin.

The vertical profile of EKE near SZ implies that eddies are active over the continental slope north of SZ, with increasing EKE from the halocline to the Atlantic Water layer (Figure 4c, the location shown in Figure 2b). The energy conversion term BCC is strong over the slope (Figure 4d), revealing the origin of eddy formation associated with the baroclinic instability of the Atlantic Water boundary current. The cyclonic boundary current also advects eddies downstream (Dmitrenko et al., 2008). In a transect downstream in the Laptev Sea sector, a core of high EKE in the Atlantic Water layer detached from the continental slope is not associated with high-energy conversion to EKE (Figures 4e and 4f), implying that some eddies are advected here by the boundary current. At this transect, strong EKE and BCC are also present at the halocline depth (Figures 4e and 4f). The map of BCC in Figure 3c reveals that energy conversion to EKE in the halocline over the continental slope in the Laptev Sea sector is higher than both the upstream and downstream slope regions. Strong local eddy formation and advection of eddies from upstream regions together can explain why rich

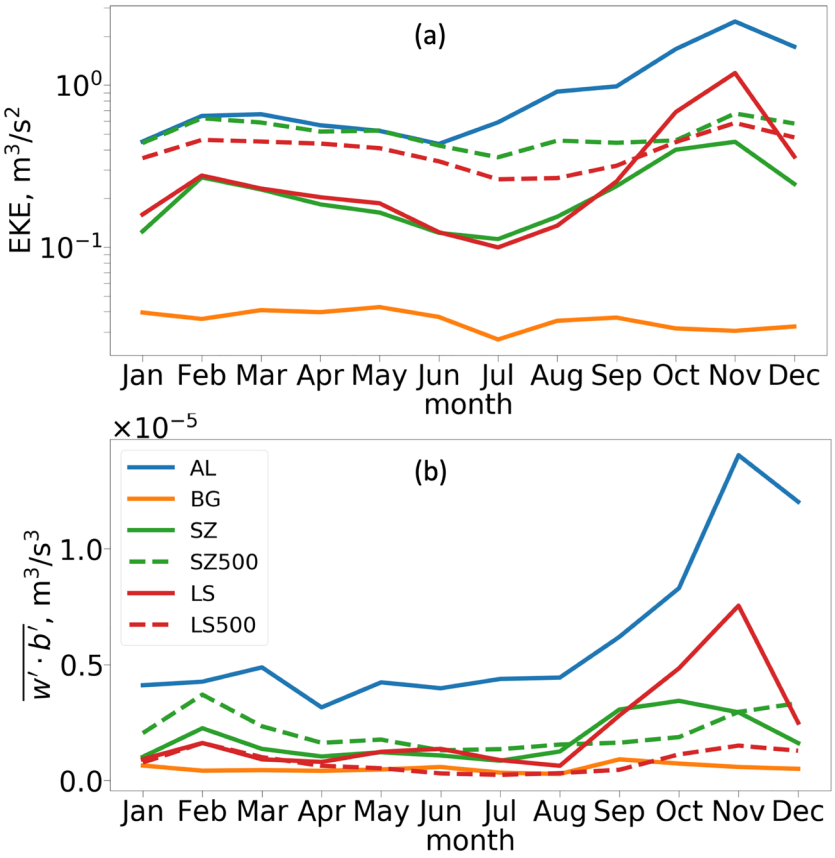


**Figure 5.** (a) Seasonal variability of vertically integrated eddy kinetic energy (EKE) averaged in chosen regions. The integration is over the depth range of 0–200 m for solid curves and 200–500 m for dashed curves. The regions are indicated in Figure 2b. (b) The same as (a) but for the energy conversion term $\overline{w' \cdot b'}$. In (a) the log10 scale is used.

eddies are present over the continental slope in the Laptev Sea sector in observations (Dmitrenko et al., 2008; Pnyushkov et al., 2018; Woodgate et al., 2001).

### 3.3. Seasonality of EKE

The EKE averaged over the upper 200 m reveals clear seasonal changes over the continental slopes off the Alaskan coast (Figure 5a). It has a maximum in fall and a minimum in late spring, consistent with the seasonal variability of the baroclinic energy conversion (Figure 5b). von Appen and Pickart (2012) compared the configurations of shelfbreak current between observed Pacific Summer Water and Pacific Winter Water at 152°W. They found that energy conversion to EKE is significantly stronger with warm water (particularly the Alaskan Coastal Water present in late summer and fall) than with Pacific Winter Water (present in spring). The simulated seasonal variation in the BCC is consistent with the finding of von Appen and Pickart (2012).

The Canada Basin is populated with anticyclonic eddies, many of which are suggested to be formed through baroclinic instability of the shelfbreak jet (Manley & Hunkins, 1985; Timmermans et al., 2008; Zhao & Timmermans, 2015; Zhao et al., 2014). We do find that anticyclones dominate in the halocline of the Canada Basin in our simulation (not shown), consistent with the aforementioned observations and previous numerical simulations (Chao & Shaw, 1996; Spall et al., 2008). At the initial stage of eddy formation, the meander is characterized by a dipole pair with a shallow cyclone and an anticyclone below it, whereas the shallow cyclone decays faster due to surface drag exerted by sea ice, resulting in the predominance of anticyclones (Chao & Shaw, 1996). Does the seasonal sea ice cover also determine the seasonal variability of the EKE in the upper ocean? The seasonal variability of EKE over the Alaskan continental slope shows higher values in fall and winter when sea ice cover is high (Figure 5a). This implies that sea ice does not significantly

modify the seasonality of EKE, which is mainly determined by the seasonality of BCC (Figures 5a and 5b). The exact impact of sea ice on EKE in different seasons and regions needs dedicated studies in future work, for example, by comparing different sources and sinks of EKE.

The seasonality of the EKE and BCC in the halocline of the eastern Eurasian Basin is very similar to that of the Alaskan coast (Figure 5). It is consistent with the seasonal changes of the shelf water. In fall and winter, the shelf water becomes cold and dense, which strengthens the ACBC and its instability after joining it. In the Atlantic Water layer, the EKE shows a seasonality similar to that in the halocline, but with a smaller magnitude. The seasonal changes of the EKE and BCC in the Beaufort Gyre are much weaker than at the slope regions.

## 4. Conclusions

This paper presents results from a decadal-scale frontier simulation with a global multiresolution ocean-sea ice model resolving the Arctic Ocean with 1-km resolution. By comparing the simulated relative vorticity and EKE with those on a 4-km resolution mesh, we conclude that at least 1-km resolution is needed in order to represent mesoscale dynamics. Using even higher resolution could further improve the eddy representation, as dynamics may still be partly damped unless grid size is as fine as one tenth of scales to resolve (Soufflet et al., 2016). We note that much higher resolution is needed to resolve eddies over the Arctic continental shelf where the deformation radius is extremely small (in places less than 1 km, Nurser & Bacon, 2014).

The 1-km simulation allowed us for the first time to obtain the spatial distribution of EKE over the whole Arctic deep basin. We identified key regions where eddies are formed and EKE is high and found that typically baroclinic instability associated with topography-steered currents is the main source of energy conversion to EKE inside the Arctic Ocean. In fact, EKE is the highest along the main currents over topography slopes, including the Eurasian and Amerasian continental slopes and the Lomonosov Ridge. The Barents Sea branch of Atlantic Water strengthens the instability of the boundary current and thus the EKE in the eastern Eurasian Basin. The EKE associated with the Beaufort/Chukchi shelfbreak jet was found to be not only the highest in the western Arctic but also higher than in other Arctic slope regions. We also found that EKE is significantly high in both the Arctic halocline and the Atlantic Water layer of the Eurasian Basin. The EKE in the interior of the Eurasian Basin and the Beaufort Gyre is high, but lower than that in slope regions. EKE constitutes a significant part (36% averaged over the deep basin) of the TKE, but their ratio varies considerably in space. The EKE at the halocline depth shows very similar seasonality over the Eurasian and Alaskan continental slopes, with maximum in fall and minimum in spring, which is linked to the seasonal changes of the boundary current instability. Our analysis provides the first Arctic-wide overview of eddy energetics.

The reported simulation belongs to an ongoing effort in developing, improving, and applying eddy-resolving Arctic Ocean simulations. In this first simulation not all diagnostics required for closed-budget energy analysis were saved from the model. Such analysis on regional scales will be conducted in future work. Employing 1 km and finer resolutions makes it possible to study dynamics of small eddies around sea ice leads and in marginal ice zones. In our simulations we have already observed eddy formation in the mixed layer under sea ice leads, but finer grid scales might be needed to better simulate such dynamics. Our multiresolution approach allows us to simulate an eddying Arctic at kilometer or subkilometer resolution in a global setup. Better resolving the Arctic Ocean while keeping its linkage to the rest of the ocean helps to improve the understanding of the role of the Arctic Ocean in the global climate. Such emerging topics will be subjects of future work.

## Data Availability Statement

The model data are available at https://doi.org/10.5281/zenodo.3761756.

**Acknowledgments**

This work is supported by the the German Helmholtz Climate Initiative REKLIM (Regional Climate Change, Q. W. and D. S.), by the projects S1 (Diagnosis and Metrics in Climate Models) and S2 (Improved parameterizations and numerics in climate models) of the Collaborative Research Centre TRR 181 "Energy Transfer in Atmosphere and Ocean" funded by the Deutsche Forschungsgemeinschaft (DFG, German Research Foundation) with Project 274762653 (N. K., P. S., S. D., and T. J.), by the FRontiers in Arctic marine Monitoring program (FRAM, C. W.), and the European Union's Horizon 2020 project APPLICATE with number 727862 (TJ). We thank the two anonymous reviewers for their very helpful comments.

## References

Aksenov, Y., Ivanov, V. V., Nurser, A. J. G., Bacon, S., Polyakov, I. V., Coward, A. C., & Beszczynska-Moeller, A. (2011). The Arctic circumpolar boundary current. *Journal of Geophysical Research*, *116*, C09017. https://doi.org/10.1029/2010JC006637

Armitage, T. W. K., Manucharyan, G. E., Petty, A. A., Kwok, R., & Thompson, A. F. (2020). Enhanced eddy activity in the Beaufort Gyre in response to sea ice loss. *Nature Communications*, *11*, 761. https://doi.org/10.1038/s41467-020-14449-z

Bashmachnikov, I. L., Kozlov, I. E., Petrenko, L. A., Glock, N. I., & Wekerle, C. (2020). Eddies in the north Greenland Sea and Fram Strait from satellite altimetry, SAR and high-resolution model data. *Journal of Geophysical Research: Oceans*, *125*, e2019JC015832. https://doi.org/10.1029/2019JC015832

Chao, S. Y., & Shaw, P. T. (1996). Initialization, asymmetry, and spindown of Arctic eddies. *Journal of Physical Oceanography*, *26*, 2076–2092.

D'Asaro, E. A. (1988). Observations of small eddies in the Beaufort Sea. *Journal of Geophysical Research*, *93*, 6669–6684.

Danilov, S., Sidorenko, D., Wang, Q., & Jung, T. (2017). The finite-volume sea ice–ocean model (FESOM2). *Geoscientific Model Development*, *10*, 765–789.

Danilov, S., Wang, Q., Timmermann, R., Iakovlev, N., Sidorenko, D., Kimmritz, M., & Schroeter, J. (2015). Finite-element sea ice model (FESIM), version 2. *Geoscientific Model Development*, *8*, 1747–1761.

Dmitrenko, I. A., Kirillov, S. A., Ivanov, V. V., & Woodgate, R. A. (2008). Mesoscale Atlantic water eddy off the Laptev Sea continental slope carries the signature of upstream interaction. *Journal of Geophysical Research*, *113*, C07005. https://doi.org/10.1029/2007JC004491

Dmitrenko, I. A., Kirillov, S. A., Ivanov, V. V., Woodgate, R. A., Polyakov, I. V., Koldunov, N., & Timokhov, L. A. (2009). Seasonal modification of the Arctic Ocean intermediate water layer off the eastern Laptev Sea continental shelf break. *Journal of Geophysical Research*, *114*, C06010. https://doi.org/10.1029/2008JC005229

Dmitrenko, I. A., Rudels, B., Kirillov, S. A., Aksenov, Y. O., Lien, V. S., Ivanov, V. V., & Barber, D. G. (2015). Atlantic water flow into the Arctic Ocean through the St. Anna trough in the northern Kara Sea. *Journal of Geophysical Research: Oceans*, *120*, 5158–5178. https://doi.org/10.1002/2015JC010804

Harrison, D. E., & Robinson, A. R. (1978). Energy analysis of open regions of turbulent flows—Mean eddy energetics of a numerical ocean circulation experiment. *Dynamics of Atmospheres and Oceans*, *2*, 185–211.

Jakobsson, M., Mayer, L., Coakley, B., Dowdeswell, J. A., Forbes, S., Fridman, B., & Weatherall, P. (2012). The International Bathymetric Chart of the Arctic Ocean (IBCAO) version 3.0. *Geophysical Research Letters*, *39*, L12609. https://doi.org/10.1029/2012GL052219

Kawaguchi, Y., Itoh, M., & Nishino, S. (2012). Detailed survey of a large baroclinic eddy with extremely high temperatures in the Western Canada basin. *Deep Sea Research Part I: Oceanographic Research Papers*, *66*, 90–102.

Koldunov, N. V., Aizinger, V., Rakowsky, N., Scholz, P., Sidorenko, D., Danilov, S., & Jung, T. (2019). Scalability and some optimization of the Finite-volumE Sea ice–Ocean Model, Version 2.0 (FESOM2). *Geoscientific Model Development*, *12*, 3991–4012.

Koldunov, N. V., Danilov, S., Sidorenko, D., Hutter, N., Losch, M., Goessling, H., & Jung, T. (2019). Fast EVP solutions in a high-resolution sea ice model. *Journal of Advances in Modeling Earth Systems*, *11*, 1269–1284. https://doi.org/10.1029/2018MS001485

Kozlov, I. E., Artamonova, A. V., Manucharyan, G. E., & Kubryakov, A. A. (2019). Eddies in the western Arctic Ocean from spaceborne SAR observations over open ocean and marginal ice zones. *Journal of Geophysical Research: Oceans*, *124*, 6601–6616. https://doi.org/10.1029/2019JC015113

Lique, C., & Steele, M. (2012). Where can we find a seasonal cycle of the Atlantic water temperature within the Arctic basin? *Journal of Geophysical Research*, *117*, C03026. https://doi.org/10.1029/2011JC007612

Manley, T. O., & Hunkins, K. (1985). Mesoscale eddies of the Arctic Ocean. *Journal of Geophysical Research*, *90*, 4911–4930.

Manucharyan, G., & Spall, M. (2016). Wind-driven freshwater buildup and release in the Beaufort Gyre constrained by mesoscale eddies. *Geophysical Research Letters*, *43*, 273–282. https://doi.org/10.1002/2015GL065957

Maslowski, W., Kinney, J. C., Marble, D. C., & Jakacki, J. (2008). Towards eddy-resolving models of the Arctic Ocean. In M. Hecht & H. Hasumi (Eds.), *Ocean modeling in an eddying regime* (pp. 241–264). American Geophysical Union. https://doi.org/10.1029/177GM16

Meneghello, G., Marshall, J., Cole, S., & Timmermans, M. L. (2017). Observational inferences of lateral eddy diffusivity in the halocline of the Beaufort Gyre. *Geophysical Research Letters*, *44*, 12,331–12,338. https://doi.org/10.1002/2017GL075126

Muench, R. D., Gunn, J. T., Whitledge, T. E., Schlosser, P., & Smethie, W. Jr. (2000). An Arctic Ocean cold core eddy. *Journal of Geophysical Research*, *105*, 23,997–24,006.

Nishino, S., Itoh, M., Kawaguchi, Y., Kikuchi, T., & Aoyama, M. (2011). Impact of an unusually large warm-core eddy on distributions of nutrients and phytoplankton in the southwestern Canada Basin during late summer/early fall 2010. *Geophysical Research Letters*, *38*, L16602. https://doi.org/10.1029/2011GL047885

Nurser, A. J. G., & Bacon, S. (2014). The Rossby radius in the Arctic Ocean. *Ocean Science*, *10*, 967–975.

Padman, L., Levine, M., Dillon, T., Morison, J., & Pinkel, R. (1990). Hydrography and microstructure of an Arctic cyclonic eddy. *Journal of Geophysical Research*, *95*, 9411–9420. https://doi.org/10.1029/JC095iC06p09411

Pickart, R. S., Torres, D. J., & Fratantoni, P. S. (2005). The east Greenland spill jet. *Journal of Physical Oceanography*, *35*, 1037–1053.

Pnyushkov, A., Polyakov, I. V., Padman, L., & Nguyen, A. T. (2018). Structure and dynamics of mesoscale eddies over the Laptev Sea continental slope in the Arctic Ocean. *Ocean Science*, *14*, 1329–1347.

Regan, H., Lique, C., Talandier, C., & Meneghello, G. (2020). Response of total and eddy kinetic energy to the recent spinup of the Beaufort Gyre. *Journal of Physical Oceanography*, *50*, 575–594. https://doi.org/10.1175/JPO-D-19-0234.1

Scholz, P., Sidorenko, D., Gurses, O., Danilov, S., Koldunov, N., Wang, Q., & Jung, T. (2019). Assessment of the finite-volume sea ice-ocean model (FESOM2.0)—Part 1: Description of selected key model elements and comparison to its predecessor version. *Geoscientific Model Development*, *12*, 4875–4899.

Soufflet, Y., Marchesiello, P., Lemarié, F., Jouanno, J., Capet, X., Debreu, L., & Benshila, R. (2016). On effective resolution in ocean models. *Ocean Modelling*, *98*, 36–50.

Spall, M. A., Pickart, R. S., Fratantoni, P. S., & Plueddemann, A. J. (2008). Western Arctic shelfbreak eddies: Formation and transport. *Journal of Physical Oceanography*, *38*, 1644–1668.

Steele, M., Morley, R., & Ermold, W. (2001). PHC: A global ocean hydrography with a high quality Arctic Ocean. *Journal of Climate*, *14*, 2079–2087.

Timmermans, M. L., Toole, J., Proshutinsky, A., Krishfield, R., & Plueddemann, A. (2008). Eddies in the Canada basin, Arctic Ocean, observed from ice-tethered profilers. *Journal of Physical Oceanography*, *38*, 133–145.

Tsujino, H., Urakawa, S., Nakano, H., Small, R. J., Kim, W. M., Yeager, S. G., & Yamazaki, D. (2018). JRA-55 based surface dataset for driving ocean–sea-ice models (JRA55-do). *Ocean Modelling*, *130*, 79–139. https://doi.org/10.1016/j.ocemod.2018.07.002

von Appen, W. J., & Pickart, R. S. (2012). Two configurations of the western Arctic shelfbreak current in summer. *Journal of Physical Oceanography*, *42*, 329–351.

von Appen, W. J., Schauer, U., Hattermann, T., & Beszczynska-Möller, A. (2016). Seasonal cycle of mesoscale instability of the West Spitsbergen Current. *Journal of Physical Oceanography*, *46*, 1231–1254.

Wang, Q., Danilov, S., Jung, T., Kaleschke, L., & Wernecke, A. (2016). Sea ice leads in the Arctic Ocean: Model assessment, interannual variability and trends. *Geophysical Research Letters*, *43*, 7019–7027. https://doi.org/10.1002/2016GL068696

Wang, Q., Danilov, S., Sidorenko, D., Timmermann, R., Wekerle, C., Wang, X., & Schröter, J. (2014). The Finite Element Sea Ice-Ocean Model (FESOM) v.1.4: Formulation of an ocean general circulation model. *Geoscientific Model Development*, *7*, 663–693.

Wang, Q., Marshall, J., Scott, J., Meneghello, G., Danilov, S., & Jung, T. (2019). On the feedback of ice–ocean stress coupling from geostrophic currents in an anticyclonic wind regime over the Beaufort Gyre. *Journal of Physical Oceanography*, *49*, 369–383.

Wang, Q., Wekerle, C., Danilov, S., Koldunov, N., Sidorenko, D., Sein, D., & Jung, T. (2018). Arctic sea ice decline significantly contributed to the unprecedented liquid freshwater accumulation in the Beaufort Gyre of the Arctic Ocean. *Geophysical Research Letters*, *45*, 4956–4964. https://doi.org/10.1029/2018GL077901

Wang, Q., Wekerle, C., Danilov, S., Sidorenko, D., Koldunov, N., Sein, D., & Jung, T. (2019). Recent sea ice decline did not significantly increase the total liquid freshwater content of the Arctic Ocean. *Journal of Climate*, *32*, 15–32.

Wang, Q., Wekerle, C., Danilov, S., Wang, X., & Jung, T. (2018). A 4.5 km resolution Arctic Ocean simulation with the global multi-resolution model FESOM 1.4. *Geoscientific Model Development*, *11*, 1229–1255.

Wang, Q., Wekerle, C., Wang, X., Danilov, S., Koldunov, N., Sein, D., & Jung, T. (2020). Intensification of the Atlantic water supply to the Arctic Ocean through fram strait induced by Arctic sea ice decline. *Geophysical Research Letters*, *47*, e2019GL086682. https://doi.org/10.1029/2019GL086682

Watanabe, E., Onodera, J., Harada, N., Honda, M. C., Kimoto, K., Kikuchi, T., & Kishi, M. J. (2014). Enhanced role of eddies in the Arctic marine biological pump. *Nature Communications*, *5*, 3950. https://doi.org/10.1038/ncomms4950

Wekerle, C., Wang, Q., Danilov, S., Schourup-Kristensen, V., von Appen, W. J., & Jung, T. (2017). Atlantic water in the nordic seas: Locally eddy-permitting ocean simulation in a global setup. *Journal of Geophysical Research: Oceans*, *122*, 914–940. https://doi.org/10.1002/2016JC012121

Woodgate, R. A., Aagaard, K., Muench, R. D., Gunn, J., Björk, G., Rudels, B., & Schauer, U. (2001). The Arctic Ocean boundary current along the Eurasian slope and the adjacent Lomonosov Ridge: Water mass properties, transports and transformations from moored instruments. *Deep Sea Research Part I: Oceanographic Research Papers*, *48*, 1757–1792.

Woodgate, R. A., Aagaard, K., Swift, J. H., Smethie Jr., W. M., & Falkner, K. K. (2007). Atlantic water circulation over the Mendeleev Ridge and Chukchi Borderland from thermohaline intrusions and water mass properties. *Journal of Geophysical Research*, *112*, C02005. https://doi.org/10.1029/2005JC003416

Zhao, M., & Timmermans, M. L. (2015). Vertical scales and dynamics of eddies in the Arctic Ocean's Canada Basin. *Journal of Geophysical Research: Oceans*, *120*, 8195–8209. https://doi.org/10.1002/2015JC011251

Zhao, M., Timmermans, M. L., Cole, S., Krishfield, R., Proshutinsky, A., & Toole, J. (2014). Characterizing the eddy field in the Arctic Ocean halocline. *Journal of Geophysical Research: Oceans*, *119*, 8800–8817. https://doi.org/10.1002/2014JC010488

Zhao, M., Timmermans, M. L., Cole, S., Krishfield, R., & Toole, J. (2016). Evolution of the eddy fields in the Arctic Ocean's Canada Basin, 2005–2015. *Geophysical Research Letters*, *43*, 8106–8114. https://doi.org/10.1002/2016GL069671